Surface Loops Adjacent to the Cation-Binding Site of the Complement Factor B von Willebrand Factor Type A Module Determine C3b Binding Specificity[†]

Danny S. Tuckwell,[‡] Yuanyuan Xu,[§] Peter Newham,[‡] Martin J. Humphries,[‡] and John E. Volanakis*[,§]

Wellcome Trust Centre for Cell-Matrix Research, School of Biological Sciences, University of Manchester, Stopford Building, Oxford Road, Manchester M13 9PT, U.K., and Division of Clinical Immunology and Rheumatology, Department of Medicine, University of Alabama at Birmingham, Birmingham, Alabama 35294

Received December 27, 1996; Revised Manuscript Received March 10, 1997[⊗]

ABSTRACT: The interaction of factor B with C3b deposited on the surface of pathogens is the first step in the activation of the alternative complement pathway. The role of the von Willebrand factor type A (VWFA) module of factor B in this interaction has been investigated by generating three chimeras, Ch1−Ch3, in which surface loops of the VWFA module flanking the cation-binding residues were replaced by the corresponding sequences of C2, a factor B-like molecule which does not bind C3b. The location of the three loops was inferred from a homology model based on the structure of the integrin αM VWFA module [Ch1, βA−α1 loop; Ch2, α3−α4 loop; and Ch3, βD−α5 loop; Lee, J.-O., et al. (1995b) *Cell 80,* 631−638]. The function of the chimeras was studied by means of hemolytic assays and assays of the individual steps of the alternative complement pathway, i.e., binding to the C3b analogue cobra venom factor and factor D cleavage. These experiments showed that Ch1 and Ch3 define regions that are involved in C3b binding whereas Ch2 does not appear to be involved in binding specificity. The inability of Ch1 to register the enhancement of cobra venom factor binding normally seen after factor D cleavage suggested that the βA−α1 loop mediates the conformational regulation of ligand binding affinity. Homology modeling of the chimeras has been used to visualize the surface structures which potentially define the C3b binding site.

The alternative pathway of complement activation allows recognition and neutralization of pathogens through the deposition of opsonic C3 derivatives and the production of anaphylatoxins, chemotactic factors, and membrane attack complexes. The first step in this pathway is the covalent attachment of C3b to pathogen surfaces, followed by binding of factor B which forms the complex C3bB. Binding to C3b renders factor B susceptible to the proteinase factor D, resulting in liberation of an N-terminal fragment of B, Ba, and formation of C3bBb. In this form, factor B expresses serine proteinase activity against C3, and therefore, the C3bBb complex is a C3 convertase.

Factor B is a modular protein composed of, from the N terminus, three complement control protein (CCP)[1] modules, a von Willebrand factor type A (VWFA) module, and a serine proteinase domain (Horiuchi et al., 1993; Mole et al., 1984). The same structure is also seen for the related protein C2 which forms the C3 convertase of the classical pathway. In factor B, the CCP modules make up the bulk of the Ba fragment cleaved off by factor D, while the two C-terminal domains comprise Bb. Electron microscopy studies have indicated that factor B has a three-lobed structure and that one lobe (Ba) is lost on factor D cleavage (Smith et al., 1984). Binding sites for C3b have been reported for all three regions [e.g., Ba, Ueda et al. (1987), Pryzdial and Isenman (1987), and Hourcade et al. (1995); VWFA module, Sánchez-Corral et al. (1990) and Hourcade et al. (1995); proteinase domain, Lambris and Müller-Eberhard (1984) and Williams and Sim (1996)], but while interactions involving the Ba region are not in doubt, electron microscopy studies of C3bBb indicate that only one of the two domains of Bb interacts with C3b (Smith et al., 1984). Therefore, the precise roles of the VWFA module and the proteinase domain in binding to C3b are currently unclear.

VWFA modules are found in a range of proteins, including certain integrin α subunits and some collagens, as well as factor B and C2 (Colombatti et al., 1993). Ligand-binding properties have been demonstrated for the VWFA modules of C2, von Willebrand factor, and integrins (Horiuchi et al., 1991; Cruz et al., 1993; Randi & Hogg, 1994; Tuckwell et al., 1995), suggesting that the factor B VWFA module could also be involved in binding to C3b. The recently determined crystal structure of the integrin αM (CD11b) VWFA module has shown that it contains a Mg^{2+} (Lee et al., 1995b; Figure 1A), and factor B-C3b binding is known to have a strong requirement for Mg^{2+} (Fishelson et al., 1983). Consistent with this, the putative cation-coordinating residues of C2 (Horiuchi et al., 1991) and factor B (Hourcade et al., 1995) have been shown to be critical for function. In addition, the EDTA-chelatable Mg^{2+} bound to factor B becomes trapped in the C3bBb complex after factor D cleavage (Fishelson et al., 1983). Taken together, the above data indicate that the factor B Mg^{2+} is intimately associated with the C3b binding site and implicate the VWFA module in

[†]Supported by a Wellcome Trust Research Travel grant (to D.S.T.) and by grants from the Wellcome Trust (to M.J.H.) and the National Institutes of Health (AI21607, to J.E.V.). J.E.V. is holder of the Anna-Lois Waters Chair of Medicine in Rheumatology.

* To whom correspondence should be addressed.

[‡] University of Manchester.

[§] University of Alabama at Birmingham.

[⊗] Abstract published in *Advance ACS Abstracts,* May 15, 1997.

[1] Abbreviations: CCP module, complement control protein module; CoVF, cobra venom factor; DMEM, Dulbecco's modified Eagle's medium; E, sheep erythrocytes; EC3b, C3b-coated E; FCS, fetal calf serum; PBS, Dulbecco's phosphate-buffered saline; VWFA module, von Willebrand factor type A module; wt, wild type.

S0006-2960(96)03155-8 CCC: $14.00

direct binding to C3b. However, direct proof has yet to be presented.

In order to study the role of the VWFA module in the factor B−C3b interaction, factor B/C2 chimeras were generated, focusing on the regions surrounding the putative factor B cation-binding residues. Although factor B and C2 are related molecules, they show a strong ligand specificity and bind with mutual exclusivity to C3b and C4b, respectively, even though these latter two molecules also have similar primary structures. Therefore, through construction of factor B/C2 chimeras and assaying for ligand binding, regions which provide C3b specificity can be identified with minimal structural disruption to the factor B molecule.

Here, we report the generation and testing of three chimeras, Ch1−Ch3, corresponding to the three cation-binding loops in the αM structure. The results identify two regions that are involved in C3b ligand specificity and provide evidence that the VWFA module of factor B is involved in binding to C3b. In addition, loop βA−α1, one of the regions defined by the chimeras, appears to be involved in the transient conformational change of the VWFA module which follows cleavage of C3b-bound factor B and is associated with the sequestration of Mg^{2+}, increased affinity for C3b, and expression of proteolytic activity for C3.

MATERIALS AND METHODS

Generation of Alignments and Homology Modeling. Alignments of integrin and complement VWFA modules were constructed separately using the ClustalW alignment program (Higgins et al., 1992) with default parameters (integrin sequences: α1, rat, chicken, human; α2, human, bovine; αE, human, mouse; αL, human, mouse; αM, human, mouse; and αX, human; complement sequences: factor B, human, lamprey, mouse, pig, *Xenopus*; and C2, human, mouse). Manual adjustments to the alignments were carried out where necessary using VISTAS (Perkins & Attwood, 1995). To assist in the alignment of the two sequence sets to give the final alignment, secondary structure predictions were carried out for both the complement and integrin sequences using PHD (Rost & Sander, 1993). A smaller version of this final alignment, showing the key sequences, is given in Figure 1B. The full alignment can be obtained from the authors. Sequence manipulations were carried out on the BBSRC SEQNET facility (Daresbury, Cheshire, U.K.) or with programs run on a Silicon Graphics 4D 240/GTX workstation.

Integrin αM VWFA module domain crystal coordinates (Lee et al., 1995b) were the kind gift of J.-O. Lee and R. Liddington. Homology modeling (Greer, 1991) was carried out using Quanta packages (MSI, Waltham, MA) and CHARM (Brooks et al., 1985). Factor B and integrin αM were aligned as described above, and the factor B residues were superposed onto the αM coordinates accordingly (the Mg^{2+} present in the crystal structure was deliberately omitted from the modeling). Small insertions or deletions in factor B relative to αM (one or two residues) were modeled by adding residues or annealing loop ends followed by local minimization. The backbone coordinates for larger insertions were modeled by searching the QUANTA fragment data base to give best matches between the Cα−Cα distance for the template termini at the site of the insertion and the Cα−Cα distance for the N and C termini of the fragment. The optimal fragment from a list of matches was chosen on the basis of the backbone likely to give the most appropriate side chain accessibilities for the factor B amino acids to be inserted. The whole model was then examined for improper contacts and bond angles. Where appropriate, side chain conformations were replaced with optimal conformations from a rotamer library (Ponder & Richards, 1987) and bad conformations were locally minimized. At this stage, chimeras Ch1−Ch3 were built from the factor B model by replacing the factor B sequence with the appropriate C2 sequence followed by checking of the altered regions against the rotamer library where necessary. All models were then minimized using steepest descent and adopted-basis Newton Raphson calculations.

Determination of electrostatic potential at the surface of the molecule was carried out within QUANTA using the method of Connolly (1983), with a probe radius of 1.4 Å.

Production and Expression of Factor B Chimeras. Mutagenesis of factor B was carried out to produce three factor B/C2 chimeras, Ch1−Ch3, corresponding to the loops flanking the cation binding residues: the βA−α1 loop (Ch1), the α3−α4 loop (Ch2), and the βD−α5 loop (Ch3) (Figures 1A and 2). The factor B cDNA clone BHL4-1 described by Horiuchi et al. (1993) was subcloned into the *Eco*RI site of the expression vector pRC/CMV (Invitrogen, San Diego, CA) and used as the wild type (wt) for the production of chimeric constructs. Ch1−Ch3 were constructed by means of mutagenic oligonucleotides (Table 1) according to the method of Zoller and Smith (1983) as modified by Kunkel (1985). All mutations were verified by dideoxynucleotide sequencing (Tabor & Richardson, 1987). All oligonucleotides were synthesized by using a model 394 DNA/RNA synthesizer (Applied Biosystems, Foster City, CA). Wild type or mutant cDNA was used to transiently transfect 4×10^6 COS cells by electroporation as described (Horiuchi et al., 1993). After 72 h, the culture supernatants, containing recombinant factor B molecules, were harvested and stored at −20 °C. Yields of recombinant proteins were determined by quantitative ELISA, as described (Horiuchi et al., 1993).

Biosynthetic Labeling and Immunoprecipitation. Sixty hours after transfection, COS cells were washed and incubated with Met-free DMEM at 37 °C for 10 min and then pulsed with [^{35}S]Met (Dupont-New England Nuclear, Boston, MA; 250 μCi/mL DMEM at 3 mL/plate) for 30 min. Radioactive medium was then removed, and the cells were washed and incubated with complete medium for 3 h. Medium containing labeled factor B was harvested, and the cells were lysed as described (Tsukamoto et al., 1996). Radiolabeled factor B was immunoprecipitated using polyclonal anti-Bb IgG/*Staphylococcus areus* complex and analyzed by 7.5% SDS−PAGE and autoradiography as described (Tsukamoto et al., 1996).

Hemolytic Assays. C3 (Gresham et al., 1986) and factor D (Volanakis & Macon, 1987) were purified as described. Properdin was purchased from Sigma Chemical Co. Sheep erythrocytes (E) carrying C3b (EC3b) were prepared by the method of Ueda et al. (1987). To remove sialic acid, EC3b (5×10^9) were washed, resuspended in 1 mL of 0.05 M sodium acetate and 0.13 M NaCl at pH 6.5, and incubated with 10 μL of type X neuraminidase (10 units/mL; Sigma Chemical Co., St. Louis, MO) for 30 min at 37 °C. Desialylated EC3b were then used for factor B hemolytic assays performed as described (Ueda et al., 1987).

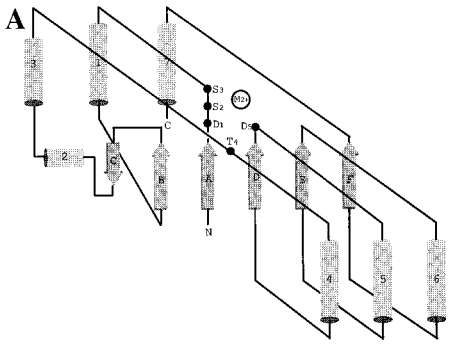

B

```
                    10        20        30        40        50        60
Xtal          --βA--        ------α1-------      ---βB----   βC-   --α2
Coord              * * *
PHD(int)     BBBBBB        aAAAAAAAAAAAAAAAA      bbBBBBBBbbbBBBBBbb
aM HUMAN     DSDIAFLIDGSGSIIPHDFRRMKEFVSTVMEQLKK--SKTLFSLMQYSEEFRIHFTFKEF
aL HUMAN     NVDLVFLFDGSMSLQPDEFQKILDFMKDVMKKLSN--TSYQFAAVQFSTSYKTEFDFSDY
aE HUMAN     GTEIAIILDGSGSIDPPDFQRAKDFISNMMRNFYEKCFECNFALVQYGGVIQTEFDLRDS
a2 HUMAN     LIDVVVVCDESNSIYP--WDAVKNFLEKFVQGLDIGPTKTQVGLIQYANNPRVVFNLNTY
C2 HUMAN     HLNLYLLLDCSQSVSENDFLIFKESASLMVDRIFSFEINVSVAIITFASEPKVLMSVLND
FB HUMAN     SMNIYLVLDGSDSIGASNFTGAKKCLVNLIEKVASYGVKPRYGLVTYATYPKIWVKVSEA
PHD(comp)     bBBBBBb          aAAAAAAAAAAAAaabbbbbbBBBBBBBb   bBBBBBb
Ch1          ...YLVLDCSQSVSENNFTGA...

                    70        80        90       100       110       120
Xtal          ---     -α3--               -----α4-----                --βD
Coord                                  *
PHD(int)           aaAAAAAAAaa           aAAAAAAAAAA aaaa            BBB
aM HUMAN     VKWK--DPDALLKPITQL---LG-RTHTATGIRKVVREL-FNITN-----GARKNAFKIL
aL HUMAN     QNNP--NPRSLVKHVKHM---LL-LTNTFGAINYVATEV-FREEL-----GARPDATKVL
aE HUMAN     QDVM--ASLARVQNITQV---GS-VTKTASAMQHVLDSI-FTSSH-----GSRRKASKVM
a2 HUMAN     KTKE--EMIVATSQTSQY---GGDLTNTFGAIQYARKYA-YSAAS-----GGRRSATKVM
C2 HUMAN     NSRDMTEVISSLENANYKDHENGTGTNTYAALNSVYLMMNNQMRLLGMETMAWQEIRHAI
FB HUMAN     DSSNADWVTKQLNEINYEDHKLKSGTNTKKALQAVYSMMSWPDDVP---PEGWNRTRHVI
PHD(comp)        aAAAAAAAAa             aAAAAAAAAAAAAA              BBB
Ch2          ...NADWVISSLENANYKDHEQGTGTNTK...

                   130       140       150       160       170       180
Xtal          ----                ----α5----         --βE--             ---
Coord             *
PHD(int)     BBBb                 aaa   aaaaa      aabbbbbbbb         aAA
aM HUMAN     VVITDGEKF--GDPL----GYEDVIPEADREG------VIRYVIGVGDAFR-----SEKS
aL HUMAN     IIITDGEAT---D--------SGNIDAAKD--------IIRYIIGIGKHFQ-----TKES
aE HUMAN     VVLTDGGIF--EDPL----NLTTVINSPKMQG------VERFAIGVGEEFK-----SART
a2 HUMAN     VVVTDGESH---DGS----MLKAVIDQCNHDN------ILRFGIAVLGYLNRNALDTKNL
C2 HUMAN     ILLTDGKSNMGGSPKTAVDHIREILNINQK----RNDYLDIYAIGVGKLD--------VD
FB HUMAN     ILMTDGLHNMGGDPITVIDEIRDLLYIGKDRKNPREDYLDVYVFGVGPL---------VN
PHD(comp)    BBBb          aaAAAAAAAAAAa             bBBBBBb
Ch3          .LMTDGKSNMGGSPITVID...

                   190       200       210       220
Xtal          α6---         -βF-   ------α7------
PHD(int)     AAAAAAA          bb   aAAAAAAAAAAAAAaabbbb
aM HUMAN     RQELNTIASKPP-RDHVFQVNNFEALKTIQNQLREKIFAIEG
aL HUMAN     QETLHKFASKPA-SEFVKILDTFEKLKDLFTELQKKIYVIEG
aE HUMAN     ARELNLIASDPD-ETHAFKVTNYMALDGLLSKLRYNIISMEG
a2 HUMAN     IKEIKAIASIPT-ERYFFNVSDEAALLEKAGTLGEQIFSIEG
C2 HUMAN     WRELNELGSKKDGERHAFILQDTKALHQVFEHMLDVSKLTDT
FB HUMAN     QVNINALASKKDNEQHVFKVKDMENLEDVFYQMIDESQ-SLS
PHD(comp)     aaaAAa          bBBb   aAAAAAAAAAaaa     b
```

FIGURE 1: VWFA module structure and sequence alignments. (A) Exploded diagram of the integrin αM VWFA module (Lee et al., 1995b) displayed to show its three-layer α−β−α structure. α-Helices are shown as cylinders and β-strands as arrows. The divalent cation (magnesium) is shown as M^{2+}, and the five coordinating residues (D_1, S_2, S_3, T_4, and D_5) are also marked. (B) Multiple alignment of complement factor B, C2 and integrin VWFA modules, and chimeras Ch1−Ch3 in the region of the factor B/C2 substitutions (substituted residues underlined). Conserved residues are shaded. This alignment represents the summary of a larger alignment (not shown) which itself combines alignments of the integrin and complement VWFA modules (see Materials and Methods). Secondary structure predictions carried out for the large alignments of integrin (int) and complement (comp) proteins using the PHD algorithm (Rost & Sander, 1993) are also shown (α-helix, A, >82% expected average accuracy, a, 72% expected accuracy; β-strand, B, >82% expected average accuracy, b, 72% expected accuracy), as is the secondary structure derived from the αM crystal (Xtal) and the residues in αM which coordinate the magnesium ion (Coord).

Cobra Venom Factor (CoVF) Binding Assays. Binding of recombinant factor B to CoVF was determined by using a solid phase assay. Microtiter plates were coated with 10 μg/mL CoVF (Quidel, San Diego, CA) in borate-buffered saline at pH 8.4 (0.1 M H_3BO_3, 25 mM $Na_2B_4O_7 \cdot 10H_2O$, and 75 mM NaCl) overnight at 4 °C and blocked with 1% BSA. Culture supernatants containing wt or chimeric factor B were dialyzed against 2.5 mM sodium 5,5-diethylbarbiturate, 0.07 M NaC1, and 1 mM $MgC1_2$ at pH 7.3 and diluted in dialyzed control culture supernatant. Factor B dilutions were added to CoVF-coated wells in the presence or absence of 1.5 μg/mL factor D and incubated for 2 h at 37 °C. Bound factor B was detected with rabbit anti-Bb IgG (20 μg/mL) and alkaline phosphatase-conjugated goat anti-rabbit IgG (Jackson Immunoresearch Laboratory, Inc., West Grove, PA). Alkaline phosphatase was developed with Sigma 104 substrate, and absorbances were read at 405 nm.

Factor D Cleavage and Immunoprecipitation of Recombinant Factor B. [^{35}S]Met-labeled factor B (300 μL) in culture supernatants was used for cleavage reactions. To this was added 3.75 μL of 2 M Tris-HCl at pH 7.4, followed by purified factor D (0.5 μg) and CoVF (10 μg). After incubation for 2 h at 37 °C, factor B and Bb were precipitated with rabbit anti-Bb IgG and were subjected to 7.5% SDS−PAGE and autoradiography.

Inhibition of N-Linked Glycosylation. Sixty hours after transfection with factor B cDNA, confluent COS cells were incubated with 10 μg/mL tunicamycin (Calbiochem, La Jolla, CA) in 2 mL of complete medium at 37 °C for 4 h followed by biosynthetic labeling with [^{35}S]Met (250 μCi/mL) as described above, in the presence of the same concentration

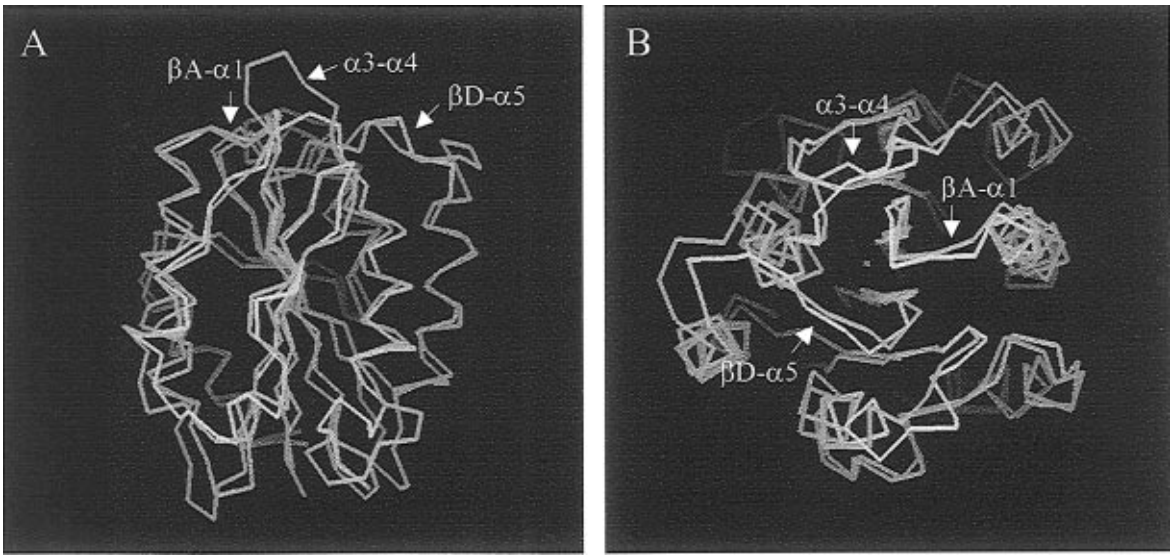

FIGURE 2: Homology modeling of the factor B VWFA module, using the structure of the αM VWFA module as the structural template. (A and B) Cα trace of the homology-modeled factor B VWFA (blue) module superposed onto the crystal structure of the integrin αM VWFA module (yellow), viewed either down the length of the β-sheet (A) or from above (B). The Mg^{2+} ion from the αM VWFA module crystal structure is shown in red. The three loops substituted in the factor B/C2 chimeras are indicated by arrows.

Table 1: Mutagenic Oligonucleotides for the Generation of Factor B Chimeras[a]

construct	factor B	C2	oligonucleotide
Ch1	913−847	840−817	5′-CTTTTTGGCTCCTGTGAAGTTATTTTCCGACACACTCTGCGAACAATCTAGCAC-CAGGTAGATGTTC-3′
Ch2	1111−1024	1041−994	5′-CTTCTTGGTGTTAGTCCCAGTTCCCTGTTCATGATCTTTATAGTTGGCATTTTCC-AGGCTGCTGATGACCCAGTCTGCATTACTGCTG-3′
Ch3	1252−1192	1188−1168	5′-CTCATCAATGACAGTAATTGGAGAGCCACCCATATTGGACTTTCCATCAGTCAT-GAGGATG-3′

[a] Oligonucleotides correspond to noncoding strand sequences. Nucleotide numbers refer to the factor B and C2 cDNA clones described in Horiuchi et al. (1993) and Bentley (1986), respectively. Underlined nucleotides indicate C2 sequence and are flanked by factor B sequence.

of tunicamycin. Immunoprecipitation with rabbit anti-Bb IgG, SDS−PAGE analysis, and autoradiography were carried out as described.

RESULTS

Production of Factor B Chimeras. Construction of factor B/C2 chimeras in the region of the cation-binding loops required comparison of the factor B and integrin αM VWFA module structure (Figure 1A). This was accomplished by a multiple alignment of factor B and C2 VWFA modules with those of the integrin α subunits. Initially, large alignments of all VWFA modules from integrin α subunits (α1, chicken, human, rat; α2, bovine, human; αE, human, mouse; αL, human, mouse; αM, human, mouse; and αX, human) and complement factor B and C2 (factor B, human, mouse, pig, *Xenopus*, lamprey; and C2, human, mouse) were constructed separately. Secondary structure predictions were produced for both alignments using PHD (Rost & Sander, 1993) and were used to give the final alignment, the essential data from which are given in Figure 1B. Comparison of the αM structure with PHD secondary structure predictions for the integrin α subunit and factor B and C2 VWFA modules (Figure 1B) suggests that all the secondary structure elements present in αM are also found in complement factor B, with the possible exception of helix α2. However, a firm statement about this helix cannot be made, as it was not predicted by PHD for the integrin VWFA modules.

In order to identify candidate regions for mutagenesis, homology modeling of the factor B VWFA module was carried out, using the integrin αM VWFA module crystal coordinates (Lee et al., 1995b) as a structural template. The integrin αM/factor B alignment used for model construction is given in Figure 1. The resulting model is given in Figure 2. Structure prediction and modeling indicated a number of differences between αM and factor B (Figures 1 and 2). Alignments suggested that the loop connecting βD and α5 was longer in the complement proteins, and secondary structure predictions suggested that helix α5 was N-terminally extended. Helical wheel plots also indicated that the α-helix periodicity could be extended N-terminally (not shown). Consequently, helix α5 of factor B was extended during the model-building process. Two other major differences were the increased lengths for the loops α3−α4 and α5−βE; however, in neither of these cases were there good grounds for extending the flanking secondary structure to accommodate the inserted sequence, and these regions were modeled as extended loops.

On the basis of the secondary structure prediction and the homology modeling, factor B/C2 chimeras Ch1−Ch3 were designed to produce molecules in which the regions flanking the three Mg^{2+}-coordinating loops of factor B were substituted with the corresponding C2 sequences. As factor B and C2 have similar primary structures and bind similar ligands, substitution of regions of factor B with C2 potentially alters the ligand specificity, while having a limited effect on the overall structure. The regions replaced in the three chimeras are given in Figure 1B: Ch1, the βA−α1 loop; Ch2, the α3−α4 loop; and Ch3, the βD−α5 loop. The cation-

Table 2: Hemolytic Activity of Wild Type and Chimeric Factor B[a]

factor B construct	hemolytic activity (units/μg) expt 1	expt 2	relative activity[b]
wild type	692	771	1.00
Ch1	51	73	0.08
Ch2	1153	992	1.48
Ch3	UD[c]	UD	−

[a] Hemolytic activities were determined by incubating C3b-coated desialylated sheep erythrocytes with factor D, properdin, and limiting quantities of wild type or chimeric factor B. C3 convertase sites were then developed by the addition of guinea pig serum diluted in EDTA-containing veronal-buffered saline at pH 7.3, followed by spectrophotometric measurement of erythrocyte lysis and calculation of hemolytic activity. [b] Specific hemolytic activity relative to wild type factor B. [c] UD, undetectable.

coordinating residues themselves were not altered by the chimeras. In Ch2, conversion of N in C2 at position 82 to Q in the chimera was considered preferable, to avoid introducing a potential glycosylation site, NGT. Chimeric factor B molecules were constructed and expressed in transiently transfected COS cells. The concentration of recombinant factor B in culture supernatants was determined by quantitative ELISA. Culture supernatants containing recombinant factor B were then used in functional assays to determine the effect of the substitutions on factor B ligand-binding specificity and associated functions.

Hemolytic Activity of Factor B Chimeras. The ability of chimeric factor B molecules to participate in the assembly of the alternative complement pathway C3/C5 convertases was tested by using hemolytic assays (Table 2). In these assays, Ch2 had specific activity equivalent to that of wt recombinant factor B. However, Ch1 had 8% wt activity, and Ch3 had less than 0.5% wt activity. The loops which were altered in Ch1 and Ch3 are therefore involved in the formation of the convertases.

Ability of Factor B Chimeras To Bind CoVF. In order to determine those steps in the assembly of the C3/C5 convertases at which the chimeras had their effect, assays which enable the individual steps of activation of the alternative pathway to be studied were used. CoVF is a C3b-like molecule from cobra venom which forms a more stable complex with factor B than C3b (Vogel & Müller-Eberhard, 1982), thus facilitating examination of its interaction with factor B. Solid phase assays (Figure 3) showed that recombinant wt factor B bound to CoVF-coated plates in a dose-dependent fashion in the absence of factor D. Ch2 behaved in a manner similar to that of wt factor B, consistent with its wt hemolytic activity. In the presence of factor D, binding of both wt and Ch2 was enhanced about 3−7-fold. Ch1 and Ch3 both showed very low levels of CoVF binding in the absence of factor D, and there was little or no increase in binding when factor D was added. Therefore, the loop substitutions in Ch1 and Ch3, but not in Ch2, have an effect on CoVF binding, which is consistent with the decreased levels of hemolytic activity seen for Ch1 and Ch3.

Factor D Cleavage of Factor B Chimeras. Binding of factor B to C3b or CoVF is a prerequisite for its cleavage by factor D. Therefore, assaying cleavage of the chimeras by factor D provides an additional measure of their binding avidity for CoVF. It also allows an evaluation of the CoVF-induced conformational changes in factor B that are thought to be necessary for the conversion of inactive "resting-state" factor D to an active serine proteinase (Volanakis & Narayana, 1996). SDS−PAGE analysis of immunoprecipitated [^{35}S]Met-labeled recombinant wt factor B and chimeras showed that Ch2 and Ch3 comigrated with wild type factor B while Ch1 ran as two bands, one with the wt molecular mass and one slightly smaller (Figure 4). After incubation with CoVF and factor D, wt factor B and Ch2, and surprisingly also Ch1, were cleaved. As expected, Ch3 was resistant to factor D cleavage.

Cleavage of Ch1 clearly produced two forms of Bb, one comigrating with wt Bb and one with a lower molecular mass. The factor B VWFA module has two potential N-linked glycosylation sites, one of which immediately follows the sequence substituted in the Ch1 chimera. The possibility that subtle conformational changes in the immediate vicinity of the substitution could have affected accessibility of the glycosylation site to processing enzymes was considered (Kornfeld & Kornfeld, 1985), as this would result in differentially glycosylated polypeptides. To investigate this possibility, transfected COS cells were treated with the N-linked glycosylation inhibitor tunicamycin before and during biosynthetic labeling of factor B. Tunicamycin treatment was found to produce a single Ch1 band with a molecular mass similar to that of the wt factor B control, demonstrating that the two Ch1 bands are due to differential N-linked glycosylation (Figure 5). However, regardless of the glycosylation pattern, both forms of Ch1 were susceptible to factor D cleavage.

Homology Modeling of wt and Chimeric Factor B Molecules. Comparative homology modeling of factor B and chimeras Ch1−Ch3 was carried out to visualize the effects of the sequence exchanges in the chimeras, and electrostatic potential surfaces were generated to examine the effects of chimera sequence substitution on the cation binding/ligand binding surface of the VWFA module (Figure 6A−D). These electrostatic potential surfaces demonstrated that major changes in charge at the cation-binding surface of factor B (a−d) occurred in all three chimeras when compared with wt factor B, and key residues could be located which apparently caused these charge changes. In Ch1, D_{12} to Q (a) and A_{16} to E (b) removed one negatively charged region and generated another at a second location. In Ch2, $K_{79}L_{80}K_{81}$ to ENG (c) removed the positive charge on this protruding loop region. In Ch3, L_{127} to K (d) generated a new positively charged site. From this, it is proposed that D_{12} (Ch1) and L_{127} (Ch3) and perhaps also A_{16} (Ch1) have important roles in defining the C3b binding site. Interestingly, despite the significant charge change c in Ch2, the results of the functional assays indicate that the loop modified in this chimera does not play a role in ligand binding specificity.

DISCUSSION

We have investigated the role of surface loops surrounding the cation-coordinating residues of the factor B VWFA module in C3b/CoVF binding specificity by generating three factor B/C2 chimeras, Ch1−Ch3. Chimera Ch2 (α3−α4 loop) had no effect on factor B ligand specificity, while Ch3 (βD−α5) could not bind CoVF/C3b and was therefore unable to initiate subsequent steps in the activation of the alternative complement pathway. Chimera Ch1 (βA−α1) also affected CoVF/C3b binding, although it did express low

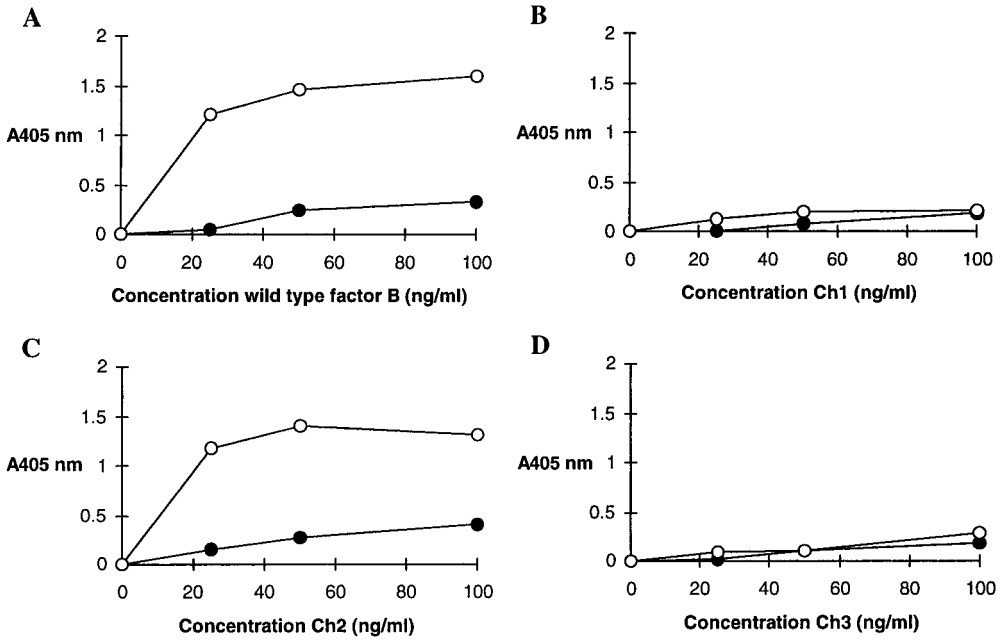

FIGURE 3: CoVF binding activity of wild type factor B and chimeras: (A) wild type, (B) Ch1, (C) Ch2, and (D) Ch3. Microtiter plates were coated with CoVF and blocked, and wild type or chimeric factor B was added in the absence (●) or presence (○) of factor D. Plates were incubated for 2 h; unbound factor B was washed off, and bound factor B was detected by ELISA.

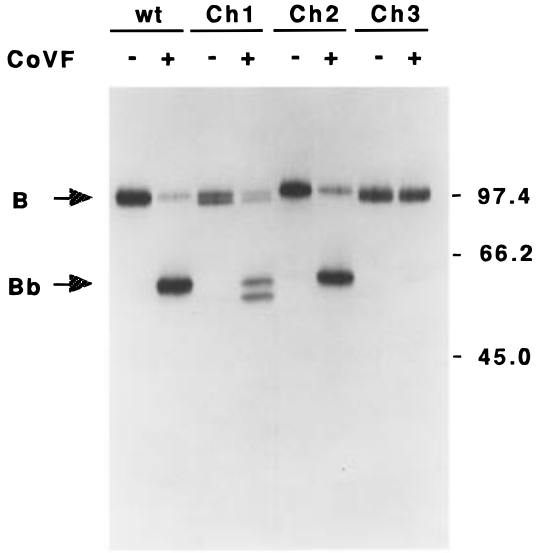

FIGURE 4: Factor D cleavage of factor B. [^{35}S]Met-labeled wt and chimeric factor B were incubated with (+) or without (−) 10 μg of CoVF in the presence of 0.5 μg of factor D, immunoprecipitated with anti-Bb IgG, and subjected to 7.5% SDS−PAGE under reducing conditions and autoradiography. Molecular masses (kilodaltons) of markers are given on the right.

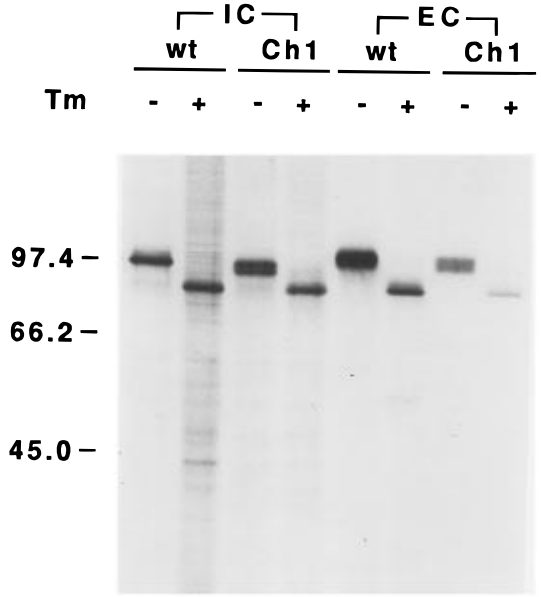

FIGURE 5: Glycosylation states of Ch1. Transfected COS cells synthesizing [^{35}S]Met-labeled wt factor B or Ch1 were treated with (+) or without (−) 10 μg/mL tunicamycin (Tm). Cell lysates (IC, intracellular) and media (EC, extracellular) were then harvested, immunoprecipitated with anti-Bb IgG, and subjected to 7.5% SDS−PAGE under reducing conditions and autoradiography. Molecular masses (kilodaltons) of markers are given on the left.

levels of hemolytic activity, and could be cleaved by factor D, suggesting that Ch1 was able to bind transiently to CoVF/C3b. Ch1 and Ch3, but not Ch2, therefore contain determinants of factor B ligand binding specificity.

The Factor B VWFA Module Provides a Binding Site for C3b. Electron microscopy studies of Bb have shown that it is a two-lobed structure and that the interaction with C3b is only mediated by a single lobe (Smith et al., 1984). There is evidence to suggest that it is the VWFA module of Bb which interacts with C3b, as mutations of its cation-binding residues block alternative pathway activation and C3b binding (Hourcade et al., 1995), and these same mutations in C2a had been previously shown to block classical pathway activation (Horiuchi et al., 1991). In addition, the VWFA module appears to be responsible for the Mg^{2+} dependence seen for Bb−C3b binding (Sánchez-Corral et al., 1990), consistent with the presence of a Mg^{2+} binding site in VWFA modules in general (Michishita et al., 1993; Lee et al., 1995a,b). However, these observations are not definitive, and there has been confusion regarding the identification of the C3b binding site in Bb, as the isolated C-terminal serine proteinase domain has also been shown to bind C3b (Lambris & Müller-Eberhard, 1984; Williams & Sim, 1997).

We have exploited the difference in ligand binding specificity between factor B and C2 to determine the C3b

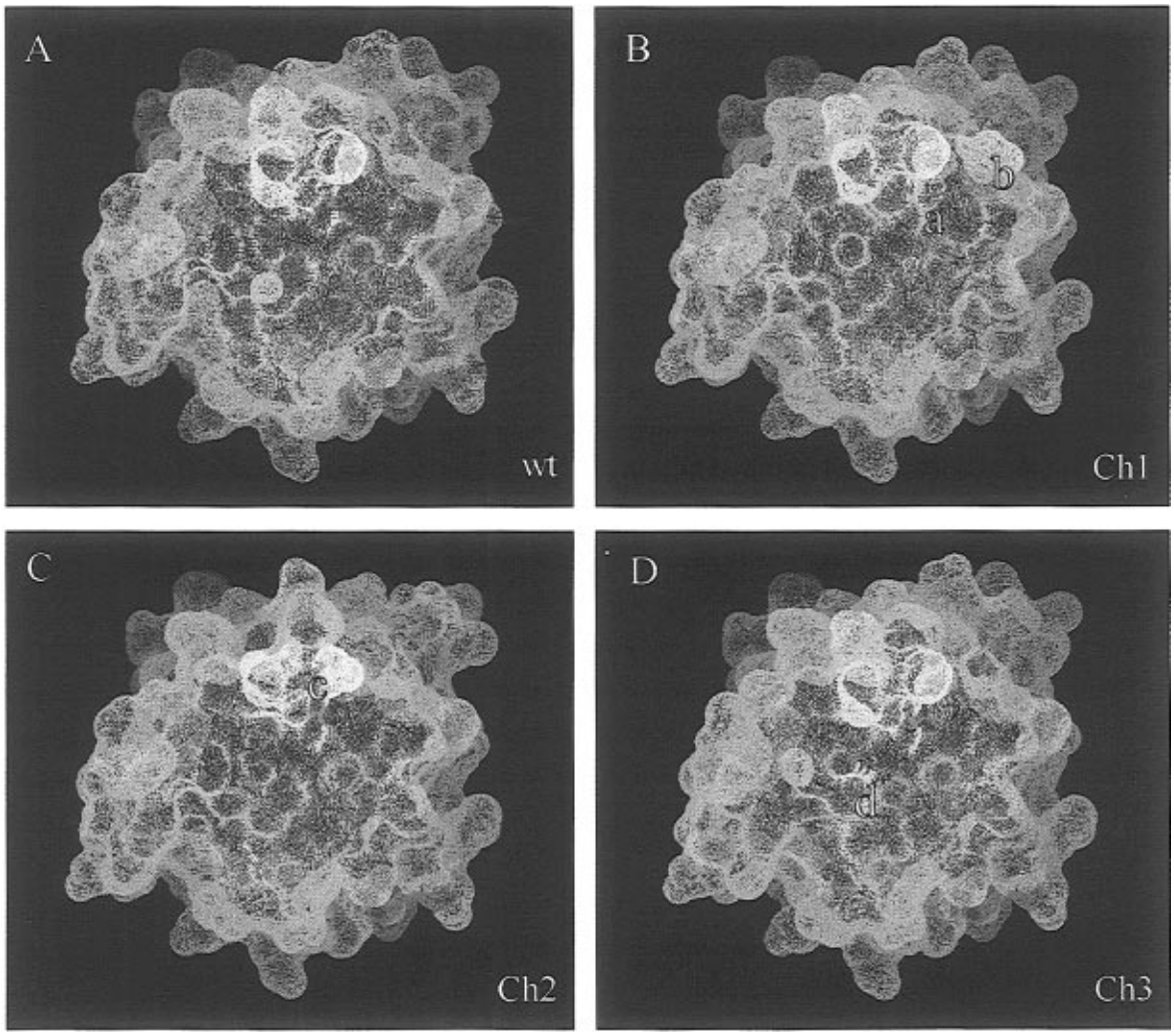

FIGURE 6: Electrostatic surface potentials of homology-modeled wt and chimeric factor B VWFA modules determined after the method of Connolly (1983): wt (A), Ch1 (B), Ch2 (C), and Ch3 (D). Molecules are viewed from above as shown in Figure 2B. a−d mark major changes in charge. The electrostatic potential ranges from positive (red) through neutral (green) to negative (blue).

binding site in factor B. The relatedness of factor B and C2 means that chimeras of the two molecules, in which short C2 sequences are substituted into factor B, can be made with minimal disruption to the three-dimensional structure of factor B, particularly, as here, when the swapped sequences are surface loops. We have shown that exchange of the βA−α1 and βD−α5 loops significantly affects binding, indicating that these regions form at least part of a C3b binding site. Significantly, only three amino acids are altered in the βD−α5 chimera (Ch3), indicating that ligand specificity is likely to be defined by a limited set of residues. Our results therefore strongly suggest that the VWFA module of Bb contains a C3b-binding site. An alternative interpretation of the results is that, through intra- or interdomain contacts, the mutations in chimeras Ch1 and Ch3 affect the conformation of distal sites participating in C3b binding. For reasons discussed in detail below, we do not favor this interpretation.

The electrostatic potential surfaces of the factor B homology models suggest that the C3b binding site has a negatively charged characteristic, as D → Q (Ch1) or L → K (Ch3) affects binding adversely. The factor B binding site of C3b has yet to be defined. A number of experiments have led to the proposal that residues 727−768 of human C3 contain the factor B binding site (Fishelson, 1991), and evidence has been presented (Taniguchi-Sidle & Isenman, 1994) for the involvement of residues E_{736} and E_{737} in binding to factor B. However, it is known that human factor B will not bind trout or *Xenopus* C3, yet recombinant chimeric human C3 molecules in which residues 727−768 were replaced with the corresponding sequence from trout or *Xenopus* still showed wt C3 convertase activity, although $E_{736}E_{737}$ was replaced by DS and YMRSS, respectively (Lambris et al., 1996). The factor B binding site would therefore appear to involve additional regions or to be located elsewhere; it may be that E_{736} and E_{737} have a supporting role in ligand binding rather than actually interacting with factor B. Further characterization of both interaction surfaces will clarify the molecular basis of the factor B−C3b interaction.

Role of Conformational Change in the Factor B VWFA Module. The binding of C3b by factor B initiates a series of conformational and structural changes in B leading to C3 and C5 convertase assembly. Initially, C3b binds factor B, forming C3bB, and this leads to a conformational change in factor B, as indicated by its ability to induce a proteolytically active conformation of factor D, a property not shared by uncomplexed factor B (Volanakis & Narayana, 1996). Cleavage by factor D, forming Bb (as C3bBb) and Ba, leads to an increase in the avidity of the C3b−Bb interaction, suggesting a conformational change in the C3b-binding site of Bb. Support for conformational changes in Bb is also

provided by observations on Ni^{2+}, which appears to bind to the same site of Bb as Mg^{2+}. Ni^{2+} bound to C3bB can be chelated by EDTA, whereas that bound to C3bBb is inaccessible (Fishelson et al., 1983). Furthermore, anti-Bb antibodies which inhibit binding of Bb to C3b but do not recognize factor B have been described (Fishelson & Müller-Eberhard, 1984). Conformational changes are apparently also involved in the expression of serine proteinase activity by factor B, as Bb resulting from dissociation of the C3bBb complex has little or no proteolytic activity (Fishelson & Müller-Eberhard, 1984). Full proteolytic activity for C3 is only expressed in the context of the C3bBb complex. By contrast, isolated Bb is more reactive by 1 order of magnitude than intact factor B against peptide thioesters corresponding to the cleavage site of C3 (Kam et al., 1987). This indicates that, in a manner similar to those of other serine proteinases, removal of the amino-terminal sequence of factor B leads to reorientation of the active center residues, associated with increased catalytic activity. However, this is not sufficient for expression of proteolytic activity, which perhaps requires C3 recognition sites only available in C3b-complexed Bb.

Factor B therefore undergoes a range of conformational changes which are central to its function. However, little is understood about either the amino acids involved in these changes or their structural basis. Although the most likely explanation for our results is that chimeras Ch1 and Ch3 represent modifications of the lingand binding site, the data also suggest that Ch1 defines a region involved in the conformational change(s) which Bb undergoes. While chimera Ch3 does not bind CoVF/C3b and therefore cannot be cleaved by factor D and initiate the subsequent steps in alternative pathway activation, chimera Ch1 is cleaved by factor D without showing the concomitant increase in CoVF binding. Therefore, Ch1 must bind CoVF, essentially below the levels of detection in our assay, and this is sufficient to permit cleavage by factor D; however, proteolysis does not induce the conformational changes necessary for increasing the avidity of Bb for CoVF. This interpretation is supported by the finding that factor D cleavage of Ch1 did not occur in the absence of CoVF (Figure 4). The residues substituted in chimera Ch1 therefore are part of the VWFA module machinery for conformational regulation of ligand affinity. This mutation could exert its effect in two ways, either by directly affecting the conformation of the C3b binding site or by affecting the mechanism of change of a nearby region. Additional support for a role of the βA$-\alpha$1 loop in conformational change is provided by the observation that oxidation of Cys_{241} in the homologous loop of C2, potentially causing conformational modification of the region, leads to increased avidity of C2a for C4b (Horiuchi et al., 1991; Parkes et al., 1983).

Factor B VWFA Module and the VWFA Module Family. VWFA modules are found in a wide range of proteins, including some integrin α subunits, as well as factor B and C2 and von Willebrand factor itself (Colombatti et al., 1993). To date, the best studied VWFA modules are those of integrin αM and αL subunits and the A1 and A3 domains of von Willebrand factor. Mutagenesis studies and epitope mapping of antifunctional antibodies indicate that, for these two sets of VWFA modules, the ligand binding sites are on the "top" cation-binding face of the molecule (Figure 1A; Ueda et al., 1994; Huang & Springer, 1995; Matsushita & Sadler, 1995). Typically, residues in the βA$-\alpha$1 and βD$-\alpha$5 loops of the integrin VWFA modules have been identified as being involved in ligand binding; this is in addition to the cation binding residues, mutation of which abrogates binding by the parent integrin (Michishita et al., 1993; Edwards et al., 1995; Kamata et al., 1995; Lee et al., 1995b). The data presented here show that the factor B VWFA module has close functional resemblances to the integrin and von Willebrand factor VWFA modules, with the C3b/CoVF binding specificity being defined by residues on the top cation-binding face of the molecule in the βA$-\alpha$1 (Ch1) and βD$-\alpha$5 (Ch3) loops.

The functional resemblance between complement and integrin/von Willebrand factor VWFA modules may also extend to the mechanisms of conformational change which the integrin VWFA modules are predicted to undergo. Crystallography of the αM VWFA module in the presence of two different cations (Mg^{2+} and Mn^{2+}) gives different structures, potentially corresponding to different ligand-binding or activation states of the module (Lee et al., 1995a,b). The main differences are seen to lie in the organization of loops on the top cation-binding face of the module, including the βA$-\alpha$1 loop, and the location of the C-terminal helix α7 relative to the rest of the molecule, as well as in the pitch of the central β-strand. In comparison, we have identified the βA$-\alpha$1 loop in factor B as potentially being involved in conformational change in factor B, and conformational change in factor B is known to be associated with changes in cation accessibility, presumably relating to the top face of the molecule. Regarding the C-terminal helix α7, proteinase domain activation may be associated with a shift in the C-terminal region of the VWFA module as the sequence linking these regions shows different susceptibilities to elastase in B and Bb (Lambris & Müller-Eberhard, 1984). The similarities in ligand binding and conformational change mechanisms between integrin and factor B VWFA modules suggest that the molecular basis of VWFA module function may be conserved across the module family.

In conclusion, we have identified regions of the factor B VWFA module which are apparently involved in binding to C3b, thereby showing that this module contains a C3b binding site. The chimera system used here represents a valuable tool for the investigation of the internal functioning of factor B, and future studies will focus on dissecting Ch1 and other chimeras, with a view toward more definitely identifying the C3b binding sites in factor B and understanding the basis of factor B ligand specificity and the function of VWFA modules.

ACKNOWLEDGMENT

The authors are grateful for the assistance of Dr. Richard Krumdieck. We are also grateful to Andy Brass for critical reading of the manuscript and to Paula Kiley for expert secretarial assistance.

REFERENCES

Bentley, D. R. (1986) *Biochem. J. 239*, 339−345.

Brooks, B. R., Bucceroli, R. B., Olafson, B. D., States, D. J., Swaminathan, S., & Karplus, M. (1985) *J. Comput. Chem. 4*, 187−217.

Colombatti, A., Bonaldo, P., & Doliana, R. (1993) *Matrix 13*, 297−306.

Connolly, M. L. (1983) *Science 221*, 709−713.

Cruz, M. A., Handin, R. I., & Wise, R. J. (1993) *J. Biol. Chem. 268*, 21238−21245.
Edwards, C. P., Champe, M., Gonzales, T., Wessinger, M. E., Spencer, S. A., Presta, L. G., Berman, P. W., & Bodary, S. C. (1995) *J. Biol. Chem. 270*, 12635−12640.
Fishelson, Z. (1991) *Mol. Immunol. 28*, 545−552.
Fishelson, Z., & Müller-Eberhard, H. J. (1984) *J. Immunol. 132*, 1425−1429.
Fishelson, Z., Pangburn, M. K., & Müller-Eberhard, H. J. (1983) *J. Biol. Chem. 258*, 7411−7415.
Greer, J. (1991) *Methods Enzymol. 202*, 239−252.
Gresham, H. D., Matthews, D. F., & Griffin, F. M. (1986) *Anal. Biochem. 154*, 454−459.
Higgins, D. G., Bleasby, A. J., & Fuchs, R. (1992) *Comput. Appl. Biosci. 8*, 189−191.
Horiuchi, T., Macon, K. J., Engler, J. A., & Volanakis, J. E. (1991) *J. Immunol. 147*, 584−589.
Horiuchi, T., Kim, S., Matsumoto, M., Watanabe, I., Fujita, S., & Volanakis, J. E. (1993) *Mol. Immunol. 30*, 1587−1592.
Hourcade, D. E., Wagner, L. M., & Oglesby, T. J. (1995) *J. Biol. Chem. 270*, 19716−19722.
Huang, C., & Springer, T. A. (1995) *J. Biol. Chem. 270*, 19008−19016.
Kam, C.-M., McRae, B. J., Harper, J. W., Niemann, M. A., Volanakis, J. E., & Powers, J. C. (1987) *J. Biol. Chem. 262*, 3444−3451.
Kamata, T., Wright, R., & Takada, Y. (1995) *J. Biol. Chem. 270*, 12531−12535.
Kornfeld, R., & Kornfeld, S (1985) *Annu. Rev. Biochem. 54*, 631−634.
Kunkel, T. A. (1985) *Proc. Natl. Acad. Sci. U.S.A. 82*, 488−492.
Lambris, J. D., & Müller-Eberhard, H. J. (1984) *J. Biol. Chem. 259*, 12685−12690.
Lambris, J. D., Lao, Z., Oglesby, T. J., Atkinson, J. P., Hack, C. E., & Becherer, J. D. (1996) *J. Immunol. 156*, 4821−4832.
Lee, J.-O., Bankston, L. A., Arnaout, M. A., & Liddington, R. C. (1995a) *Structure 3*, 1333−1340.
Lee, J.-O., Rieu, P., Arnaout, M. A., & Liddington, R. C. (1995b) *Cell 80*, 631−638.
Matsushita, T., & Sadler, J. E. (1995) *J. Biol. Chem. 270*, 13406−13414.
Michishita, M., Videm, V., & Arnaout, A. (1993) *Cell 72*, 857−867.
Mole, J. E., Anderson, J. K., Davison, E. A., & Woods, D. E. (1984) *J. Biol. Chem. 259*, 3407−3412.
Parkes, C., Gagnon, J., & Kerr, M. A. (1983) *Biochem. J. 213*, 201−209.
Perkins, D. N., & Attwood, T. K. (1995) *J. Mol. Graphics 13*, 73−75.
Ponder, J. W., & Richards, F. M. (1987) *J. Mol. Biol. 193*, 775−791.
Pryzdial, E. L. G., & Isenman, D. E. (1987) *J. Biol. Chem. 262*, 1519−1525.
Randi, A. M., & Hogg, N. (1994) *J. Biol. Chem. 269*, 12395−12398.
Rost, B., & Sander, C. (1993) *J. Mol. Biol. 232*, 584−599.
Sánchez-Corral, P., Anton, L. C., Alcolea, J. M., Marqués, G., Sánchez, A., & Vivanco, F. (1990) *Mol. Immunol. 27*, 891−900.
Smith, C. A., Vogel, C.-W., & Müller-Eberhard, H. J. (1984) *J. Exp. Med. 159*, 324−329.
Tabor, S., & Richardson, C. C. (1987) *Proc. Natl. Acad. Sci. U.S.A. 84*, 4767−4771.
Taniguchi-Sidle, A., & Isenman, D. E. (1994) *J. Immunol. 153*, 5285−5301.
Tsukamoto, H., Tousson, A., Marchase, R. B., & Volanakis, J. E. (1996) *J. Immunol. 156*, 4901−4908.
Tuckwell, D. S., Calderwood, D. A., Green, L. J., & Humphries, M. J. (1995) *J. Cell Sci. 108*, 1629−1637.
Ueda, A., Kearney, J. F., Roux, K. H., & Volanakis, J. E. (1987) *J. Immunol. 138*, 1143−1149.
Ueda, T., Rieu, P., Brayer, J., & Arnaout, M. A. (1994) *Proc. Natl. Acad. Sci. U.S.A. 91*, 10680−10684.
Vogel, C.-W., & Müller-Eberhard, H. J. (1982) *J. Biol. Chem. 257*, 8292−8299.
Volanakis, J. E., & Macon, K. J. (1987) *Anal. Biochem. 163*, 242−246.
Volanakis, J. E., & Narayana, S. V. L. (1996) *Protein Sci. 5*, 553−564.
Williams, S. C., & Sim, R. B. (1997) *Mol. Immunol.* (in press).
Zoller, M. J., & Smith, M. (1983) *Methods Enzymol. 100*, 468−500.

BI963155L